Eng. Sci., 2022, **19**, 136–143

Engineered Science

DOI: https://dx.doi.org/10.30919/es8d711

Isotropic Ferromagnetic Resonances Induced by Suppressed Anisotropy in Soft Magnetic Microstructures

Lianze Ji,[1, 2,†] Xiaochen Shen,[2, 3,†] Rongzhi Zhao,[1, 2,*] Chenglong Hu,[1, 2] Xiaoyu Zhao,[2] Yixing Li,[1] Jian Zhang,[2] Wenchao Chen,[2] Yimin Chen,[1] Jamal Daoud[4] and Xuefeng Zhang[1, 2]

Abstract

The miniaturization of electronic devices has brought new challenges and opportunities due to the appearance of unusual physical effects. Especially, the in-plane anisotropy introduced during the film deposition can be not beneficial for soft magnetic applications. Herein, we demonstrated the suppression of anisotropy in soft magnetic films by constructing quasi-three-dimensional soft magnetic microstructures which include a magnetic dots array in the bottom layer and a magnetic antidot array in the top layer. It is confirmed that the in-plane anisotropy can be suppressed by the characterization of hysteresis loops, ascribed to the formation of annular stripe domains induced by the competition between exchange energy and demagnetization energy in the dots array. The resonant frequencies of patterned microstructures increase from 1.2 GHz to 3.3 GHz with the increase of external magnetic fields from 32 Oe to 160 Oe. Thus, our results provide insight for designing tree-dimensional devices without in-plane anisotropy.

Keywords: Ferromagnetic resonances; Quasi-three-dimensional; Microstructures.
Received: 26 February 2022; Revised: 19 April 2022; Accepted: 21 April 2022.
Article type: Research article.

1. Introduction

With the development of miniaturization in electronic devices, there are great demands for soft magnetic films to realize information storage with high density,[1] signal transmission with high speed[2], and energy transformation with high efficiency.[3] Benefiting from the advances in nanopatterning techniques, it is convenient to achieve the design of electronic devices with complex structures in compact and effective volumes.[4-8] For example, magnonic crystals, as one of the electromagnetic metamaterials, present promising applications in waveguides[9] and spin valves,[10] where the performance can be regulated conveniently by external magnetic fields. Effective anisotropy can be induced by changing the preparation technique of materials[11] and using flexible substrates.[5,12] However, when the size of microstructures becomes extremely small, unusual physical phenomena can appear due to the confined effect, thermal effect, high electric field, and so on.[13-16] An alternative way is to design three-dimensional (3D) device architectures by stacking magnetic layers along the out-of-plane direction.[17,18] Especially, the magnetic film with antidot arrays can achieve the splitting ferromagnetic resonances for applications of electromagnetic compatibility with the wide band,[19] ascribed to the design of period shape anisotropy. Combined with the antidot arrays and dot arrays, the resonant frequencies can be expected to be widened furtherly.

On the other hand, inhomogeneous ground states of magnetic domains can be nucleated in the units of microstructures due to confined effects when the bias field is below the saturation field,[8,19] ascribed to the competition between exchange energy, Zeeman energy, demagnetization energy, and magnetocrystalline anisotropy energy.[5,19-21] Exciting physics can be brought when the structures are extended into 3D structures. For example, both transversal and longitudinal domain walls can be induced in curved magnets,[22] where the special structure can produce an additional effective Dzyaloshinskii-like energy.[23] Abundant

[1] *Key Laboratory for Anisotropy and Texture of Materials (MOE), School of Materials Science and Engineering, Northeastern University, Shenyang 110819, China.*
[2] *Institute of Advanced Magnetic Materials, College of Materials and Environmental Engineering, Hangzhou Dianzi University, Hangzhou 310012, China.*
[3] *Key Laboratory of Materials Modification by Laser, Ion and Electron Beams, School of Materials Science and Engineering, Dalian University of Technology, Dalian 116023, China.*
[4] *Galenvs Sciences Inc., Quebec, H3E1M3, Canada.*
[†] *These authors contributed equally.*
[*] *E-mail:* zhaorz@hdu.edu.cn (R. Zhao)

ferromagnetic resonances can be excited by the collective dynamics of magnetic moments,[24-26] which brings rich degrees of freedom for the design of electronic devices. However, the directional arrangement of magnetic moments can induce the anisotropy of ferromagnetic resonances, leading to the deterioration of soft magnetic properties.

Herein, we achieved the isotropic ferromagnetic resonances in a quasi-3D soft magnetic film by the process of microfabrication, including a magnetic dots array in the bottom layer and a magnetic antidot array in the top layer. Directional stripe domains are observed in continuous films, where the in-plane anisotropy can be confirmed by the characterization of hysteresis loops and anisotropic ferromagnetic resonances can be induced. Such an anisotropy can be suppressed in the quasi-3D soft magnetic microstructure, ascribed to the formation of annular stripe domains in the dots array of the bottom layer. The isotropic resonant frequencies of patterned microstructures increase from 1.2 GHz to 3.3 GHz with the increase of external magnetic fields from 32 Oe to 160 Oe. Thus, our results can provide insight for designing soft magnetic materials with isotropic ferromagnetic resonances.

2. Experimental part

The fabrication of patterned microstructures are made by using photoetching (URE-2000/35A, Institute of Optics and Electronics, China), as shown in Fig. 1(a). The photoresist is AZ5214 and the thickness is 1.2 μm, which is coated on silicon (Si) substrates and exposed to ultraviolet light with a wavelength of ~365 nm under the cover of a patterned mask. In Fig. 1(b), the patterned photoresist is obtained after the process of development. DC magnetron sputtering is used to deposit the magnetic films of $Fe_{20}Ni_{80}$ with a thickness of 150 nm in an ultrahigh vacuum of 5×10^{-6} Pa, where the deposition rate is 0.30 nm/s by the measurement of a calibrated crystal monitor. The sputtering process is initiated to 0.4 Pa by flowing Argon gas. Consequently, a quasi-3D soft magnetic microstructure is constructed without the process of removing the photoresist (Fig. 1(c)). Samples are cut into the size of 5×5 mm^2 for the characterization of magnetic properties.

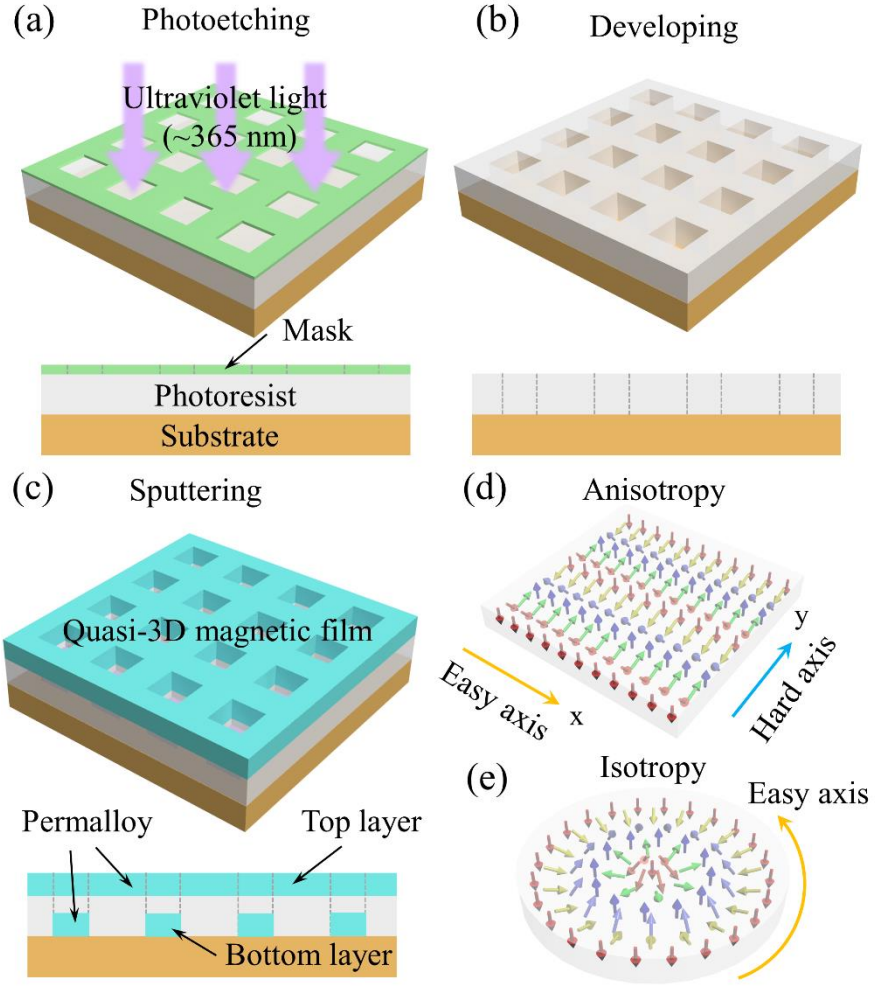

Fig. 1 Illustration of the preparation of quasi-3D soft magnetic microstructures. The process of (a) photo etching, (b) developing, and (c) sputtering. (d) The stripe domains formed in continuous films and the antidot layer of the bottom layer. In-plane anisotropy is induced by the directional magnetic moments. (e) The annular stripe domains formed in the dots layer of the bottom layer. In-plane isotropy can appear in such a magnetic domain.

The images of microstructures are obtained by field emission scanning electron microscopy (SEM, JSM IT500 HR, JEOL, Japan) and the crystal structures of the deposited films are analyzed by using X-ray diffraction (XRD, Smart Lab 9 KW, Rigaku, Japan) with Cu-Kα radiation (λ = 1.5418 Å; 30 kV). The hysteresis loops are measured by using a magnetic property measurement system (MPMS3, Quantum Design Inc., US) with in-plane external magnetic fields. The magnetic domains are characterized by using magnetic force microscopy (MFM, NanoWizard 4-NanoScience, JPK Instruments AG, Germany) and the scanning process is carried out with standard magnetic Co/Cr-coated cantilevers (Multi75M-G, Budgetsensors, force constant of 3 N/m). The ferromagnetic resonant spectra are characterized by a home-built one-port spectrometer,[27] where samples are placed in the cavity of a short-circuit microstrip line and microwave cavity of a short-circuit microstrip line, and microwave signals are collected by a vector network analyzer (VNA, Keysight N5224B, US). The stripe domains can be formed in continuous films (Fig. 1(d)), where similar magnetic domains can also be observed in the antidot array of the top layer. In the dots array of the bottom layer, the stripe domains can arrange along the direction of patterned edges (Fig. 1(e)) by the competition between exchange energy and demagnetization energy,[5,24] where the in-plane anisotropy can disappear. Such a magnetic structure is similar to the target skyrmion[28] which can nucleate in multilayer magnetic films with interfacial Dzyaloshinskii-Moriya interaction and can be extended to kπ-skyrmions with the increase of annular domain walls.[29]

3. Results and discussion

Figures 2(a)-(c) show the SEM images of patterned microstructures, which are hexagon, square, and triangle arrays, respectively. The length of patterns in the dots array is denoted by *d*. The distances between patterns are marked by *p* (x-direction) and *w* (y-direction), respectively. The values also are summarized in Fig. 2(d) and the units are micrometers (μm). The XRD in Fig. 2(e) shows the (1 1 1) peak of $Fe_{20}Ni_{80}$ at 2θ = 44.2°. Directional stripe domains are observed in continuous films (Fig. 2(f)), which can induce an in-plane anisotropy. The magnetic structures of antidot arrays and dot arrays can be observed clearly in Figs. 2(f)-(i). Annular stripe domains can be formed in dot arrays (the bottom layer) because of the shape anisotropy,[20] which are marked by the inner regions of white dotted lines in Figs. 2(g)-(i). Such a magnetic domain can be expected to suppress the in-plane anisotropy by the symmetrical magnetic structures. In antidot arrays (the top layer), the stripe domains arrange along the edge of antidot arrays due to the synergistic effect of the shape anisotropy and the interfacial strain.[5]

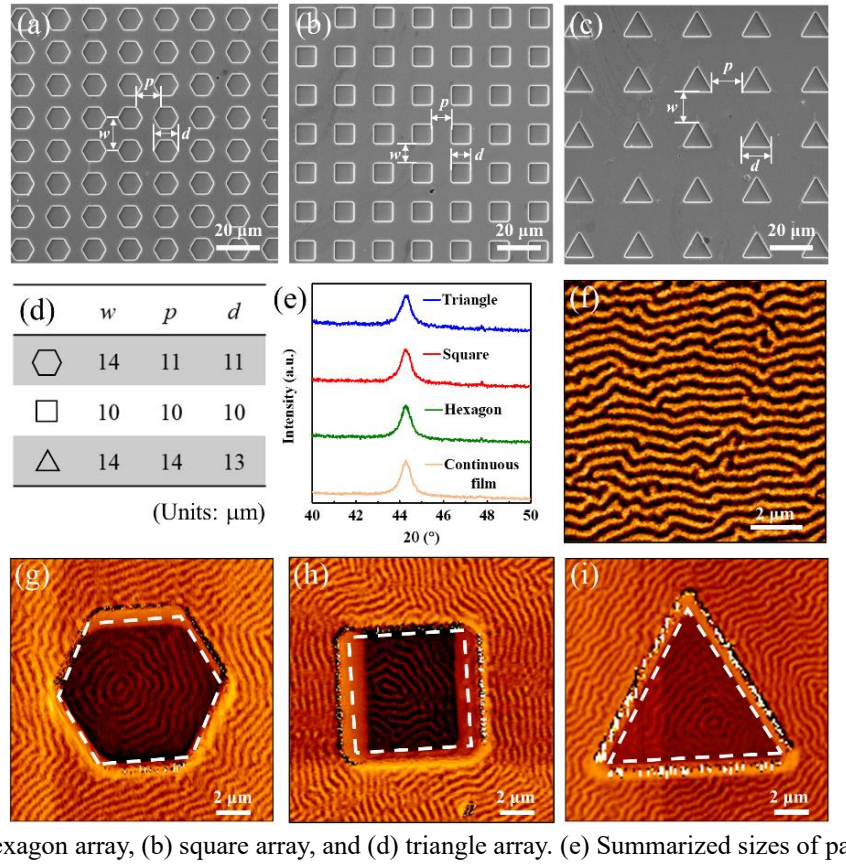

Fig. 2 SEM images of (a) hexagon array, (b) square array, and (d) triangle array. (e) Summarized sizes of patterns by *p*, *w,* and *d*. (f) XRD characterization of continuous films and patterned films. Magnetic domains of (f) continuous films, (g) hexagon, (h) square, and (i) triangle arrays. The inner regions and outer regions divided by white dotted lines show the magnetic domain of the dots array in the bottom layer and the antidot array in the top layer, respectively.

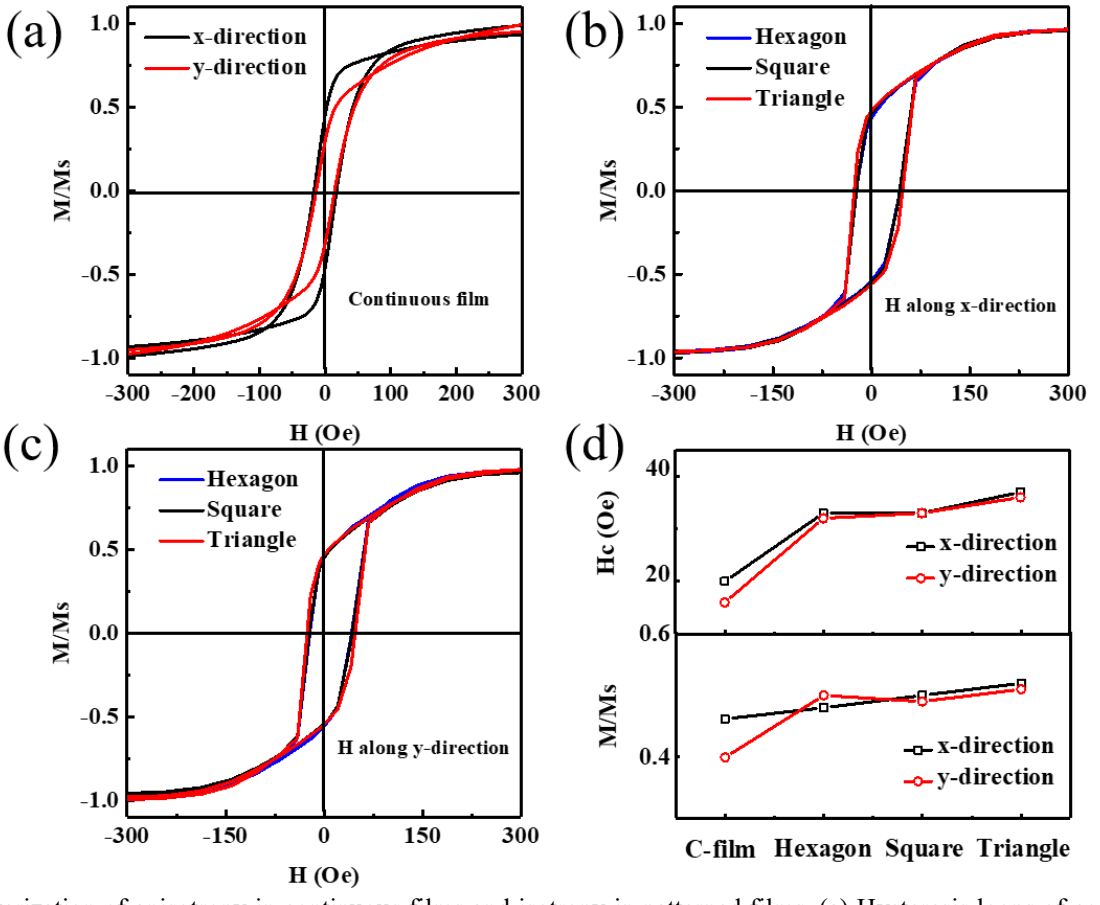

Fig. 3 Characterization of anisotropy in continuous films and isotropy in patterned films. (a) Hysteresis loops of continuous films with in-plane anisotropy. Hysteresis loops of patterned films along the (b) x-direction and (c) y-direction. (d) The summary of remanent magnetization (M_r/M_s) and coercivity (H_c) for continuous films and patterned films. The continuous film is marked by the symbol of C-film.

Then, the in-plane hysteresis loops are measured along the x-direction and y-direction of magnetic films to confirm the suppression of in-plane anisotropy in patterned films, as shown in Fig. 3. The directions of x and y are consistent with the marks in Fig. 1(d). The in-plane anisotropy of continuous films is observed in Fig. 3(a), where the coercivities (H_c) are 20 Oe and 16 Oe along the x-direction and y-direction, respectively. The remanent magnetization (M_r/M_s) is 0.46 and 0.40 along the x-direction and y-direction, respectively. The anisotropy in continuous films can originate from the formation of oblique columnar crystals in the preparation process,[11] which can induce the directional arrangement of magnetic moments and can be used to design nonreciprocal electric devices.[30] However, the in-plane anisotropy can be suppressed by designing patterned microstructures, as shown in Figs. 3(b)-(c). The H_c are both 32 Oe and M_r/M_s are both 0.5 for the measurement along the x-direction (Fig. 3(b)) and y-direction (Fig. 3(c)), ascribed to the formation of annular stripe domains in the dots array of the bottom layer and intermediate state in the antidots array of the top layer. The results also are summarized in Fig. 3(d), where the continuous film is marked by the symbol of C-film. It is obvious that the in-plane anisotropy is suppressed in patterned microstructures. It should be noted that the increase of coercivity in patterned magnetic films could result from the formation of the effective anisotropy induced by the interfacial strain between the photoresist and magnetic films.[5]

Figures 4(a) and 4(b) show the real (μ') and imaginary (μ'') parts of the permeability of magnetic films without external magnetic fields, respectively. Along the x-direction, continuous films have a resonant frequency (f_r) of 1.38 GHz with μ' of 2200-21000 at $f < f_r$ and μ'' of 17000 at f_r. An anisotropic ferromagnetic resonance is observed along the y-direction, where the resonant frequency (f_r) is1.25 GHz with μ' of 2600-14000 at $f < f_r$ and μ'' of 26000 at f_r. A low damping constant can be expected due to the rapid increase of μ'.[31] For the patterned films, the resonant frequencies increase to 1.4 GHz, 1.37 GHz, and 1.38 GHz for hexagon, square, and triangle arrays, respectively. No obvious anisotropy of resonant frequencies is observed in these patterned films. Compared with continuous films, the permeabilities of patterned films have a decrease of real (9000, 10000, and 7000 for hexagon, square, and triangle arrays, respectively) and imaginary (11000, 13000, and 8000 for hexagon, square, and triangle arrays, respectively) parts at f_r. The similar decrease can also be observed along the y-direction and such a phenomenon is consistent with the two-dimension patterned magnetic film.[31]

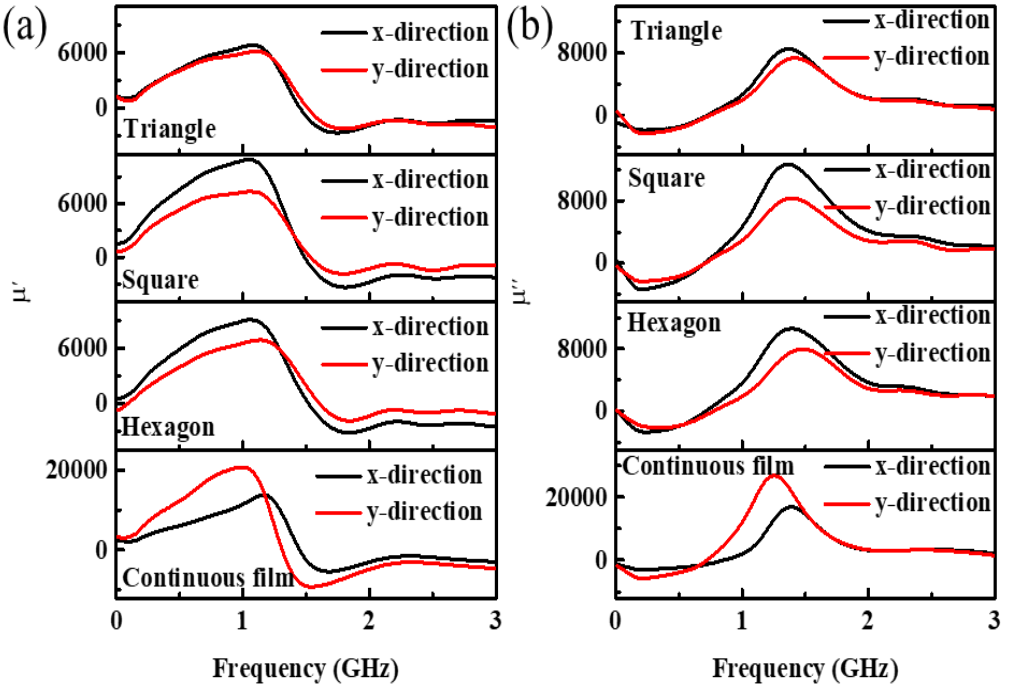

Fig. 4 Ferromagnetic resonant spectra for continuous films and patterned films. (a) Real and (b) imaginary parts of the complex permeability without an external magnetic field.

The dependence of permeabilities on external magnetic fields (H) along the x-direction and y-direction is shown in Fig. 5 and Fig. 6, respectively. There is a decrease of f_r when the magnetic field is low than 32 Oe. Then, a linear increase is

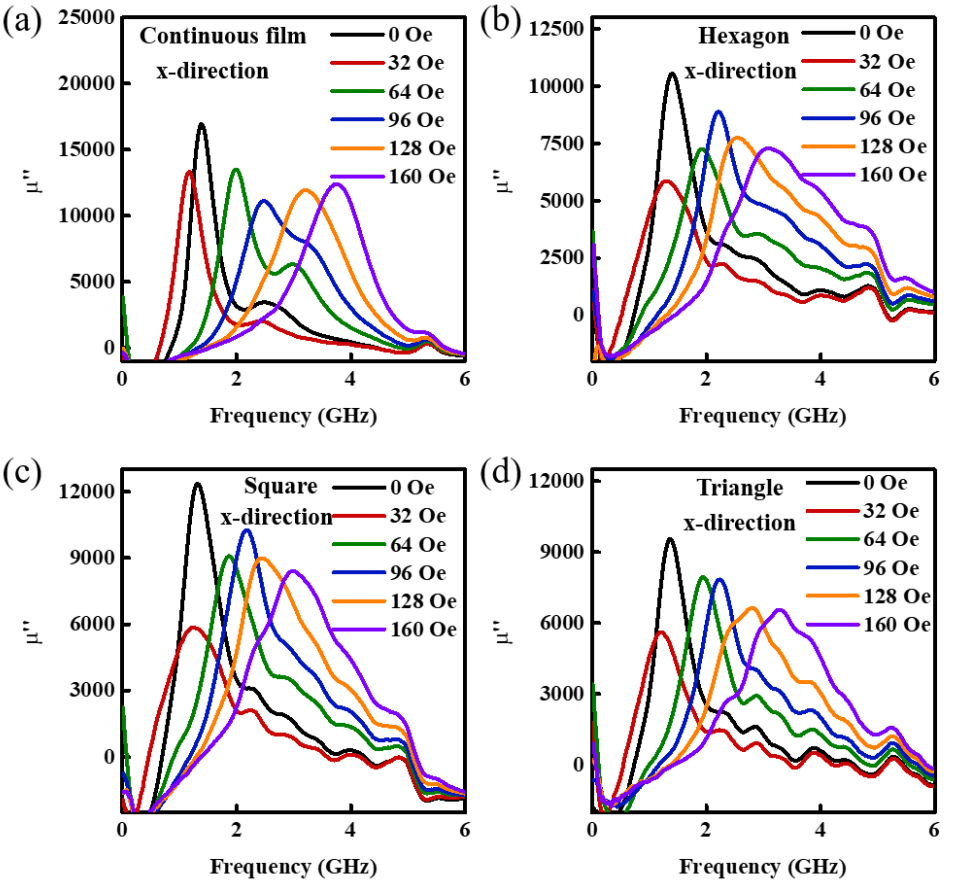

Fig. 5 Imaginary parts of complex permeability for continuous films and Hexagonal patterned films along the x-direction under external magnetic fields (H). (a) Continuous films. (b) Hexagonal patterns. (c) Square patterns. (d) Triangle patterns.

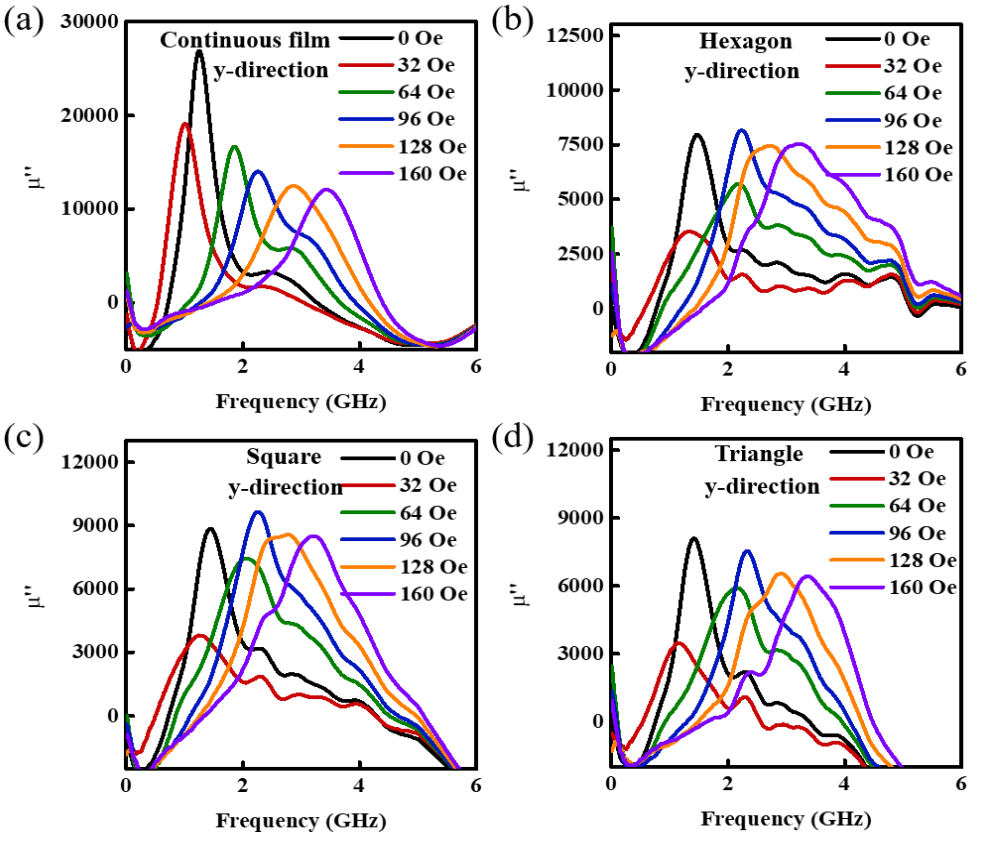

Fig. 6 Imaginary parts of complex permeability for continuous films and Hexagonal patterned films along the y-direction under external magnetic fields (H). (a) Continuous films. (b) Hexagonal patterns. (c) Square patterns. (d) Triangle patterns.

observed with the increase of magnetic fields from 32 Oe to 160 Oe. The values of μ'' of continuous films (Fig. 5(a) and Fig. 6(a)) are about two times than patterned films ((Figs. 5(c)-(d) and Figs. 6(b)-(d))). The frequencies of ferromagnetic resonances increase from 1.15 GHz to 3.75 GHz for continuous films along the x-direction (Fig. 5(a)) and from 1.0 GHz to 3.45 GHz for continuous films along the y-direction (Fig. 6(a)) with the increase of external magnetic fields from 32 Oe to 160 Oe. For the patterned films, the isotropic ferromagnetic resonances are achieved due to the suppression of in-plane anisotropy. With the increase of external magnetic fields from 32 Oe to 160 Oe, the frequencies increase from 1.3 GHz to 3.1 GHz (Fig. 5(b) and Fig. 6(b)), from 1.2 GHz to 3.0 GHz (Fig. 5(c) and Fig. 6(c)) and from 1.2 GHz to 3.3 GHz (Fig. 5(d) and Fig. 6(d)) for hexagon, square and triangle arrays, respectively. Consistent changes are observed along the x-direction and y-direction. Thus, the anisotropy can be suppressed in comparison with continuous films by introducing the patterned microstructures.

In order to present the isotropic ferromagnetic resonances obviously, the dependence of resonant frequencies on external magnetic fields (H) along the x-direction and y-direction are shown in Figs. 7(a) and 7(b), respectively. Ferromagnetic resonant spectra are measured three times to avoid measuring errors. It is observed that there is a difference of ~0.6 GHz between continuous films and patterned films when the magnetic field along the x-direction is larger than 120 Oe (Fig. 7(c)), where the difference of frequency (f_d) is calculated by $f_r = f_p - f_c$ with the frequencies of patterned films f_p and continuous films f_c in Fig.7(a). When magnetic fields are along the y-direction, there are no differences in the frequency between continuous films and patterned films (Fig. 7(b)). Such an isotropic ferromagnetic resonance can originate from the formation of symmetrical magnetic textures along x and y directions, where the stripe domain is parallel to the edge of antidot arrays and annular stripe domains are formed in the dot arrays.

To emphasize the isotropic ferromagnetic resonances of patterned films, the differences in frequencies between the x-direction and y-direction are calculated in Fig. 7(d). The anisotropy can only be observed in continuous film and the patterned films present isotropic ferromagnetic resonances. The fluctuation near 50 Oe and 125 Oe could be induced by the intrinsic property of the test fixture, which results from the resonance of the cavity. Finally, the ferromagnetic resonance is mainly decided by the magnetic structures, where the annular stripe domain can induce isotropy ferromagnetic resonances (see Figs. 1 (d) and (e)). Thus, the isotropy ferromagnetic resonance can be observed in these magnetic films with different patterns. For example, splitting ferromagnetic resonances[19] can be observed in magnonic crystals with different patterns, where similar arc-shaped domain walls are observed in these magnetic films with different antidot arrays.

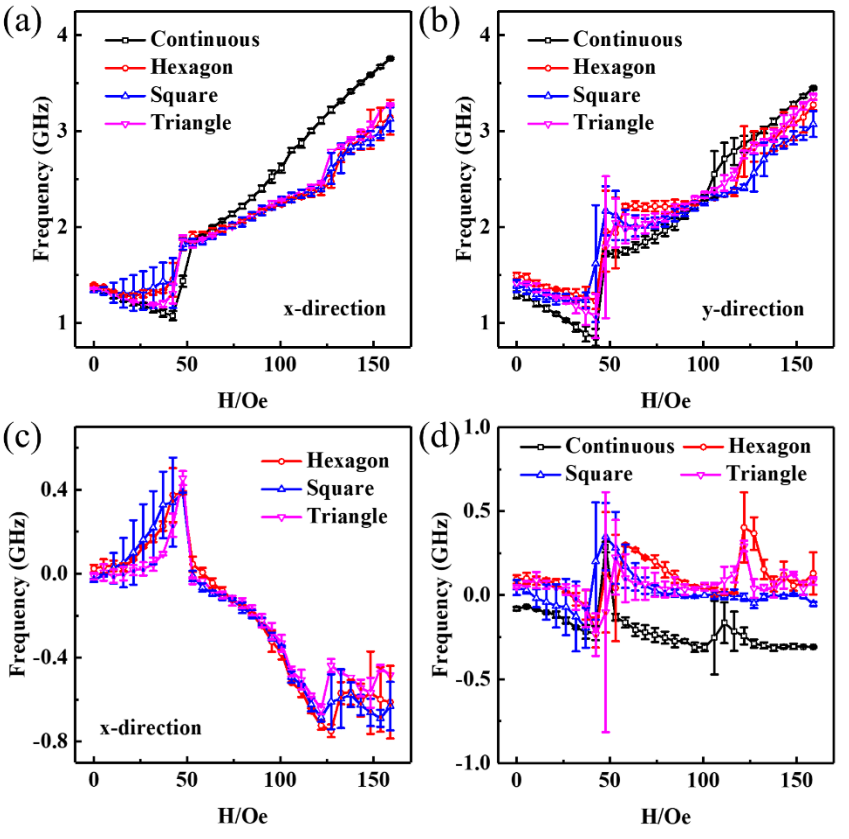

Fig. 7 Summarized ferromagnetic resonant frequencies as a function of external magnetic fields for continuous films and patterned films. The dependence of resonant frequencies along the (a) x-direction and (b) y-direction. (c) The differences of resonant frequencies between continuous films and patterned films along the x-direction. (d) The differences of resonant frequencies between the x-direction and y-direction.

4. Conclusion

In conclusion, we demonstrated the isotropic ferromagnetic resonances in quasi-3D soft magnetic films which include a magnetic dots array in the bottom layer and a magnetic antidot array in the top layer. Combined with the characterization of hysteresis loops and magnetic domains, it is confirmed that the suppression of in-plane anisotropy is ascribed to the formation of annular stripe domains in the dots array and intermediate states in the antidot array. The ferromagnetic resonant frequencies of patterned films increase from 1.2 GHz to 3.3 GHz with the increase of external magnetic fields from 32 Oe to 160 Oe and a difference of 0.6 GHz is observed in comparison with continuous films along the easy-axis direction. Thus, our results can provide insight for designing 3D architecture of electronic devices without the consideration of in-plane anisotropy.

Acknowledgments

The authors gratefully acknowledge the National Key Research and Development Program of China (2019YFE0121700), the Key Research and Development Program of Zhejiang Province (2021C01033), the Fundamental Research Funds for the Provincial Universities of Zhejiang (GK219909299001-003), the National Key Scientific Instrument and Equipment Development Project of China (51927802), and the Start-up Program of Hangzhou Dianzi University (KYS385618067).

Conflict of Interest

The authors declare no conflict of interest.

Supporting information

Not applicable.

References

[1] M. M. Waldrop, *Nature*, 2016, **530**, 144-147, doi: 10.1038/530144a.

[2] H. Zhao, Y. Shuang, M. Wei, T. J. Cui, P. D. Hougne, L. Li, *Nature Communications*, 2020, **11**, 3926, doi: 10.1038/s41467-020-17808-y.

[3] J. M. Silveyra, E. Ferrara, D. L. Huber, T. C. Monson, *Science*, 2018, **362**, eaao0195, doi: 10.1126/science.aao0195.

[4] A. Fernández-Pacheco, R. Streubel, O. Fruchart, R. Hertel, P. Fischer, R. P. Cowburn, *Nature Communications*, 2017, **8**, 15756, doi: 10.1038/ncomms15756.

[5] J. Zhang, W.-K. Lee, R. Tu, D. Rhee, R. Zhao, X. Wang, X. Liu, X. Hu, X. Zhang, T. W. Odom, M. Yan, *Nano Letters*, 2021, **21**, 5430-5437, doi: 10.1021/acs.nanolett.1c00070.

[6] J. Tang, Y. Wu, L. Kong, W. Wang, Y. Chen, Y. Wang, Y. Soh, Y. Xiong, M. Tian, H. Du, *National Science Review*, 2021, **8**, doi: 10.1093/nsr/nwaa200.
[7] J. Wang, Y. Liu, Z. Fan, W. Wang, B. Wang, Z. Guo, *Advanced Composites and Hybrid Materials*, 2019, **2**, 1-33, doi: 10.1007/s42114-018-0067-9.
[8] H. Yao, S. Wang, M. Lei, K. Bi, *Engineered Science*, 2021, **16**, 301-307, doi: 10.30919/es8d549.
[9] P. Pirro, V. I. Vasyuchka, A. A. Serga, B. Hillebrands, *Nature Reviews Materials*, 2021, **6**, 1114-1135, doi: 10.1038/s41578-021-00332-w.
[10] H. Li, Q. Zhan, Y. Liu, L. Liu, H. Yang, Z. Zuo, T. Shang, B. Wang, R.-W. Li, *ACS Nano*, 2016, **10**, 4403-4409, doi: 10.1021/acsnano.6b00034.
[11] G. Wang, C. Dong, Z. Yan, T. Wang, G. Chai, C. Jiang, D. Xue, *Journal of Alloys and Compounds*, 2013, **573**, 118-121, doi: 10.1016/j.jallcom.2013.03.245.
[12] N. N. Song, B. Y. Lv, J. Meng, Z. Z. Gong, X. D. Zhang, Q. F. Zhan, *Journal of Magnetism and Magnetic Materials*, 2021, **519**, 167510, doi: 10.1016/j.jmmm.2020.167510.
[13] P. Xie, Y. Liu, M. Feng, M. Niu, C. Liu, N. Wu, K. Sui, R. R. Patil, D. Pan, Z. Guo, R. Fan, *Advanced Composites and Hybrid Materials*, 2021, **4**, 173-185, doi: 10.1007/s42114-020-00202-z.
[14] Q. Jiang, Y. Qiao, C. J. Xiang, A. Uddin, Wu L, F. X. Qin, *Advanced Composites and Hybrid Materials*, 2022, **2**, 1-11, doi: 10.1007/s42114-021-00394-y.
[15] H. H. Hu, H. P. Liu, D. J. Zhang, J. J. Wang, G. W. Qin, X. F. Zhang, *Engineering Science*, 2018, **2**, 43-48, doi: 10.30919/es8d136.
[16] H. Cheng, Z. Lu, Q. Gao, Y. Zuo, X. Liu, Z. Guo, C. Liu, C. Shen, *Engineering Science*, 2021, **16**, 3313-340, doi: 10.30919/es8d518
[17] O. Ozatay, A. Gokce, T. Hauet, L. Folks, A. Giordano, G. Finocchio, *Physical Review Applied*, 2019, **11**, 014002, doi: 10.1103/physrevapplied.11.014002.
[18] R. Lavrijsen, J.-H. Lee, A. Fernández-Pacheco, D. C. M. C. Petit, R. Mansell, R. P. Cowburn, *Nature*, 2013, **493**, 647-650, doi: 10.1038/nature1173
[19] L. Ji, R. Zhao, X. Hu, C. Hu, X. Shen, X. Liu, X. Zhao, J. Zhang, W. Chen, X. Zhang, *Advanced Functional Materials*, 2022, **32**, 2112956, doi: 10.1002/adfm.202112956.
[20] R. Z. Zhao, C. L. Hu, L. Z. Ji, W. C. Chen, X. F. Zhang, *Science China Physics, Mechanics & Astronomy*, 2020, **63**, 1-8, doi: 10.1007/s11433-020-1529-0.
[21] R. Zhao, W. Chen, X. Zhang, *Applied Physics Letters*, 2018, **113**, 062405, doi: 10.1063/1.5042605.
[22] O. V. Pylypovskyi, V. P. Kravchuk, D. D. Sheka, D. Makarov, O. G. Schmidt, Y. Gaididei, *Physical Review Letters*, 2015, **114**, 197204, doi: 10.1103/physrevlett.114.19720.
[23] D. D. Sheka, V. P. Kravchuk, Y. Gaididei, *Journal of Physics A: Mathematical and Theoretical*, 2015, **48**, 125202, doi: 10.1088/1751-8113/48/12/125202.
[24] L. Bo, L. Ji, C. Hu, R. Zhao, Y. Li, J. Zhang, X. Zhang, *Applied Physics Letters*, 2021, **119**, 212408, doi: 10.1063/5.0072349.
[25] L. F. Lyu, J. R. Liu, H. Liu, C. T. Liu, Y. Lu, K. Sun, R. H. Fan, N. Wang, N. Lu, Z. H. Guo, E. K. Wujcik, *Engineering Science*, 2018, **2**, 26-42, doi: 10.30919/es8d615.
[26] Y. Fan, J. Finley, J. Han, M. E. Holtz, P. Quarterman, P. Zhang, T. S. Safi, J. T. Hou, A. J. Grutter, L. Liu, *Advanced Materials*, 2021, **33**, 2008555, doi: 10.1002/adma.202008555.
[27] J. Wei, J. Wang, Q. Liu, X. Li, D. Cao, X. Sun, *Review of Scientific Instruments*, 2014, 85, 054705, doi: 10.1063/1.4876598.
[28] Y. Liu, H. F. Du, M. Jia, A. Du, *Physical Review B*, 2015, **91**, 094425, doi: 10.1103/PhysRevB.91.094425.
[29] J. Jiang, Y. Wu, L. Kong, Y. Wang, J. Li, Y. Xiong, J. Tang, *Acta Materialia*, 2021, **215**, 117084, doi: 10.1016/j.actamat.2021.117084.
[30] C. Liu, S. Wu, J. Zhang, J. Chen, J. Ding, J. Ma, Y. Zhang, Y. Sun, S. Tu, H. Wang, P. Liu, C. Li, Y. Jiang, P. Gao, D. Yu, J. Xiao, R. Duine, M. Wu, C.-W. Nan, J. Zhang, H. Yu, *Nature Nanotechnology*, 2019, **14**, 691-697, doi: 10.1038/s41565-019-0429-7.
[31] X. Chen, Y. G. Ma, C. K. Ong, *Journal of Applied Physics*, 2008, **104**, 013921, doi: 10.1063/1.2953065.

Author Information

Lianze Ji *is currently a Ph. D. student in Northeastern University, China. His current research interests include the high-frequency magnetic properties of micro-nano-structured materials for the soft-magnetic alloy.*

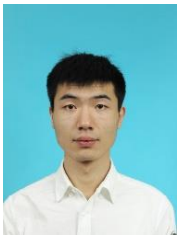

Rongzhi Zhao *is currently working in Hangzhou Dianzi University, China. His current research interests include magnetic functional materials for electronic and information technology.*